COMMUNICATION

In situ measurement of lithiation-induced stress in silicon nanoparticles using micro-Raman spectroscopy

Zhidan Zeng[a,b,c,1], Nian Liu[d,1], Qiaoshi Zeng[a,b,c], Seok Woo Lee[d], Wendy L. Mao[a,e,*], Yi Cui[d,e,**]

[a]Department of Geological Sciences, Stanford University, Stanford, CA 94305, USA
[b]Center for High Pressure Science and Technology Advanced Research (HPSTAR), Shanghai 201203, PR China
[c]HPSynC, Geophysical Laboratory, Carnegie Institution of Washington, Argonne, IL 60439, USA
[d]Department of Materials Science and Engineering, Stanford University, Stanford, CA 94305, USA
[e]Photon Science and Stanford Institute for Materials and Energy Sciences, SLAC National Accelerator Laboratory, Menlo Park, CA 94025, USA

Abstract
Stress is a long standing challenge for the applications of silicon (Si) anodes in lithium (Li) ion batteries. Nanostructured Si are important materials to address mechanical stress issues in batteries although their stress was only calculated and no experimental data are available. Using in situ Raman microscopy to monitor the shift of the first-order Raman peak of Si, we were able to measure for the first time the lithiation-induced stress in Si nanoparticles. The shift of Raman peak of Si under hydrostatic stress was calibrated via an in situ high pressure Raman experiment. We observed a tensile-to-compressive transition of the stress in Si core of nanoparticles during lithiation. At the beginning of lithiation, the reduction of the surface native oxide on the Si particle results in a tensile stress of approximately 0.2 GPa in Si. During the formation of amorphous Li_xSi in the outer layer of the nanoparticles, an increasing compressive stress up to 0.3 GPa is built up in the Si core. This stress evolution explains the cracks that developed in the amorphous Li_xSi layer during lithiation of the Si nanoparticles, and is also consistent with modeling results. These results improve our understanding of

*Corresponding author at: Department of Geological Sciences, Stanford University, Stanford, CA 94305, USA. Tel.: +1 650 723 3718; fax: +1 650 725 2199.
**Corresponding author at: Department of Materials Science and Engineering, Stanford University, Stanford, CA 94305, USA. Tel.: +1 650 723 4613; fax: +1 650725 4034.
 E-mail addresses: wmao@stanford.edu (W.L. Mao), yicui@stanford.edu (Y. Cui).
[1]These authors contributed equally to this work.

lithiation-induced stress in nanostructured Si anodes, and provide valuable information for their computational study and rational engineering.

Introduction

Lithium ion batteries (LIBs) are an important energy storage system due to their high capacity, long lifetime, environmental friendliness, etc. However, the capacities of current electrode materials are too low to meet the need of high energy density storage for portable electronics and electric vehicles applications. Therefore high capacity electrode materials are critical for next generation batteries. In terms of anode materials, Si has the highest theoretical specific capacity of 3579 mAh/g (formation of $Li_{15}Si_4$), near ten times higher than the currently used graphite (370 mAh/g) [1]. To achieve this high capacity, each Si atom hosts more than three Li ions during lithiation, forming amorphous Li_xSi (a-Li_xSi, $x = 3.4 \pm 0.2$) or crystalline $Li_{15}Si_4$ [1,2]. Alloying and de-alloying with large amount of Li ions result in dramatic volumetric changes in the Si anodes, and consequently lead to enormous internal stress during battery operation [3].

Stress in electrode materials affects the performance of LIBs in many ways [4]. It can cause fracture and pulverization of electrode materials, which lead to their loss in contact to each other or to the current collectors [5-7]. Fracture of the electrode materials also exposes fresh surfaces to the electrolyte, which consumes extra Li ions to form new solid electrolyte interphase (SEI) layers during battery cycling [8]. These two factors are the main reasons that account for the decay in capacity of LIBs. The stress status determines the failure mode of the electrode materials. For instance, a tensile stress in the core of a Si particle leads to fracture starting from the core; while a tensile stress in the outer layer of the particle causes cracks on its surface. In addition, stress would also change thermodynamics and kinetics of the electrochemical reaction in LIBs, and alter the effective potential window for electrochemical cycling [9-11].

To mitigate stress and fracture associated with battery operation, different nanostructured Si anodes have been intensively studied, e.g. nanoparticles, porous nanoparticles, nanowires, double-walled hollow tubes, core-shell, yolk-shell, pomegranate structures [12-23]. Compared with bulk Si anodes that usually fail within a few cycles, nanostructured Si anodes can maintain their integrity after hundreds of cycles [12,19,24]. This significant improvement in performance is attributed to the release of stress in the nanoscale. Although the stress in bulk Si anodes has been experimentally determined, the stress in nanostructured Si anodes has never been measured, which is crucial for understanding of their behavior and further optimization of their performance.

By measuring stress induced substrate curvature, Chon et al. determined the stress in a-Li_xSi layer of a 425–450 μm thick Si wafer (diameter 50.8 mm) [3]. They found an almost constant compressive stress of approximately 0.5 GPa in the a-Li_xSi during lithiation. The lithiation-induced stress in Si nanoparticles is expected to be different, as they show highly improved battery performance compared with their bulk counterpart. Theoretical studies suggest that the hoop stress in the a-Li_xSi layer of Si nanoparticles changes from compression to tension during lithiation, and a similar stress transition is reported in Ge nanopillars [25,26]. However, no experimental results have been available.

In this study, the lithiation-induced stress in Si nanoparticle anodes was investigated using in situ Raman microscopy. A tensile stress of 0.2 GPa was observed in Si at the beginning of lithiation, followed by a transition to a compressive stress up to 0.3 GPa upon further lithiation. These results not only reveal the stress evolution in Si nanoparticles during lithiation, but also can validate theoretical models for nanostructured Si anodes.

Experimental

Electrochemical cell fabrication

Si nanoparticles (MTI Corporation, ~100 nm) were mixed with carbon black (Super P, TIMCAL, Switzerland) and sodium carboxymethyl cellulose (Sigma-Aldrich, Mw ~90,000) with a mass ratio of 45:45:10 and stirred in deionized water overnight. A piece of stainless steel mesh (400 mesh, TWP Inc.) was dip-coated with this slurry and baked in a vacuum oven at 90 °C for >3 h to obtain a Si nanoparticles electrode. The mass of the Si nanoparticles in an electrode (ca. 0.1 mg) was determined using a microbalance (Sartorius SE2, 0.1 μg resolution).

Figure 1a and b shows the schematic and photograph of the electrochemical cell respectively. The cells were assembled using a Si nanoparticles electrode, Li metal as the counter electrode, and a Celgard separator soaked in electrolyte, similar to previous reports [27,28]. The electrolyte was 1.0 M $LiPF_6$ in 1:1 (w/w) ethylene carbonate/diethyl carbonate (BASF). The cells were assembled inside an Ar-filled glovebox and sealed in 0.11 mm thick transparent polyester pouches (Kapak Corporation). For efficient sealing of the battery cells, pretaped Ni current collectors (MTI Corporation) were used. In situ battery cycling was performed using a MTI eight-channel battery analyzer (0.002–1 mA). The voltage cutoff was set to 2.0 V and 0 V versus Li/Li^+, and the cycling rate was C/10 in terms of the theoretical capacity of Si (4200 mAh/g). A cycling rate of C/10 means charge/discharge in 10 h.

High pressure sample preparation

For in situ high pressure Raman experiment, a crystalline Si sample was loaded into a symmetric diamond anvil cell (DAC). The sample chamber was a 120 μm diameter hole
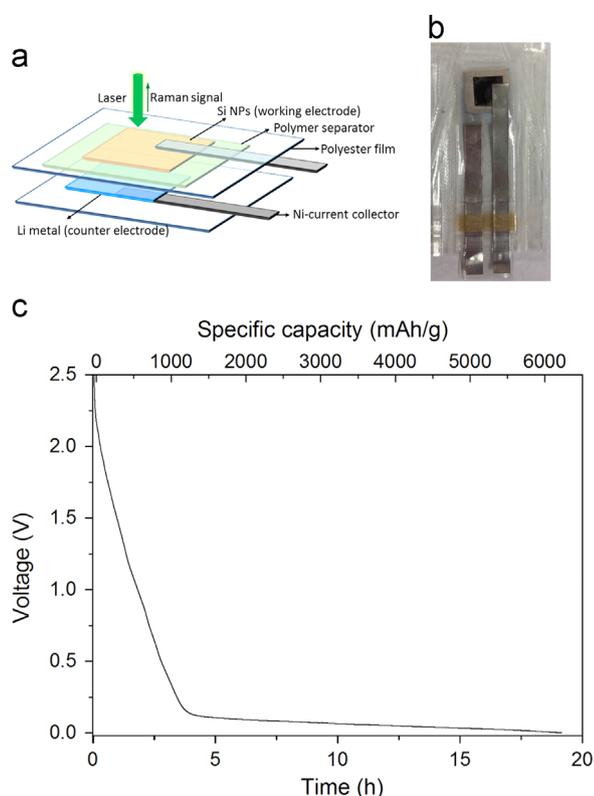
Figure 1 A schematic diagram (a) and a photograph (b) of the "transparent" half cell for in situ micro-Raman measurement. (c) Voltage as a function of time (bottom axis) and specific capacity (top axis) during galvanostatic lithiation of the Si nanoparticles at a rate of C/10.

drilled in a T301 stainless steel gasket. A tiny ruby ball was also loaded in the sample chamber as a pressure calibrant. Pressure was measured by monitoring the shift in the R1 fluorescence line of ruby [29]. Helium was loaded as the hydrostatic pressure transmitting medium using the gas loading system in the Extreme Environments Laboratory (EEL) at Stanford University.

In situ Raman measurements

We used the same Raman system for both the in situ electrochemical cell and high pressure experiment. In situ Raman measurements were carried out using a Renishaw in Via micro-Raman system with a 514.5 nm laser excitation line. A low laser power of 2.5 mW was used to minimize any thermal effects. A collection time of 30 s was used for each spectrum, for each acquisition 10 spectra were accumulated in order to reduce noise and avoid CCD saturation. The intervals between acquisitions were set to 5 min. To determine the peak position of the first-order Raman peak of Si, the peak was fit using a Voigt function after linear background subtraction.

Results and discussion

Figure 1c shows the voltage profile (electrochemical data) of the cell during galvanostatic lithiation. The voltage

profile shows an almost flat voltage plateau around 0.1 V after 4 h of discharge, implying Si starts to be electrochemically lithiated via a two-phase mechanism [30,31]. X-ray photoelectron spectroscopy results indicate the formation of the Li-Si alloy starts at the surface of Si nanoparticles at the very beginning of the plateau [32]. Before the plateau, i.e. during the first 4 h of discharge, side reactions including reduction of SiO_2 and formation of SEI occur [32,33]. The lithiation capacity goes beyond the theoretical capacity (3579 mAh/g); the extra capacity could be attributed to these side reactions due to the high specific surface area of Si nanoparticles.

Figure 2 shows a series of Raman spectra of Si nanoparticles in the working battery during lithiation. The first Raman spectrum was collected before the discharge began, in which the first-order Raman peak of crystalline Si near 520 cm^{-1} is intense. The other Raman peaks originate from either the electrolyte or the polyester pouch. The intensity of Si Raman peak stays very high in the first 4 h, followed by a sharp decrease during further lithiation. This change in peak intensity is consistent with the electrochemical reaction of Si anodes. As mentioned above, Si nanoparticles remain unreacted at the beginning, which explains the stable Raman signal of Si nanoparticles during this period. Once the lithiation of Si begins at ∼4 h (as shown in Figure 1c), the outer layer of Si nanoparticles is transformed to a-Li_xSi ($x=3.4\pm0.2$), which has a much higher conductivity than Si [2]. The high conductivity of a-Li_xSi results in a small optical skin depth (penetration depth of the laser), leading to the decrease of Si Raman peak intensity. Meanwhile, the intensities of the Raman peaks of the electrolyte and pouch remain nearly constant, indicating that the change in Si Raman peak is associated with the electrochemical reaction.

For each Raman spectrum, a Voigt function is fit to the first-order Raman peak of Si after linear background subtraction. Figure 3 shows the peak position (X_c), full-width at half-maximum (FWHM) of the peak and adjusted R^2 value of the fit as functions of the lithiation duration. The Raman peak shifts to lower wavenumber in the first 2 h, then to higher wavenumber upon further reaction (after 4 h). The FWHM of the Raman peak increases along with the lithiation, which could be attributed to the stress induced lattice
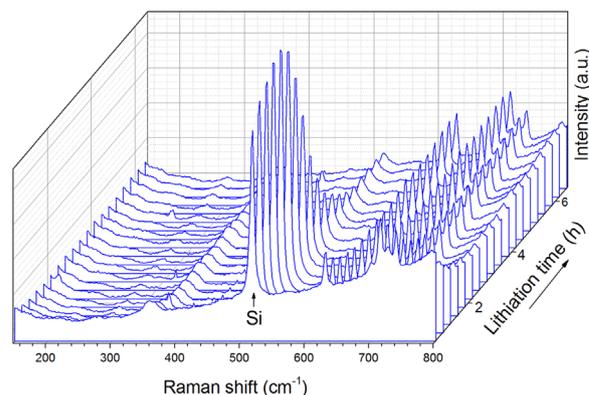

Figure 2 Selected Raman spectra of the half cell during lithiation. A laser power of 2.5 mW and a collection time of 30 s were used for each spectrum, for each acquisition 10 spectra were accumulated.

distortion [34]. The adjusted R^2 value indicates that the fit quality decreases after 4 h of discharge due to the lattice distortion as well as the decreased peak intensity.

The frequency of the first-order Raman peak of crystalline Si is sensitive to stress. In general, compressive stress will cause an increase of the Raman frequency, while tensile stress results in a decrease [34]. This makes in situ micro-Raman spectroscopy a promising approach to measure the stress in Si nanoparticles, which is otherwise difficult to determine using other methods. In order to establish the quantitative relation between the shift of the Raman peak and the stress, we measured Raman spectra of a crystalline Si sample at different hydrostatic stress (pressures) up to around 10 GPa in a DAC (see Figure S1a). Figure S1b shows the frequency of the first-order Raman peak of the Si sample as a function of compressive stress (pressure). By fitting the experimental data, the relationship between peak shift and stress is obtained as follows:

$$\Delta w/\mathrm{cm}^{-1} = -4.4\sigma/\mathrm{GPa} \tag{1}$$

where $\Delta\omega$ is the shift of Raman peak from its position at ambient pressure, and σ is the stress (negative for compressive stress, and positive for tensile stress). Thus the stress in the Si nanoparticles could be estimated according to this relation.

Figure 4a shows the calculated stress in the Si nanoparticles as a function of lithiation duration along with the voltage profile of the battery, and Figure 4b schematically shows the stress evolution. Initially, a tensile stress up to ~0.2 GPa is gradually built up in Si nanoparticles, which then saturates upon further reaction. Although the pressurized hollow sphere model exhibits compressive stress in the crystalline Si core of the spherical particle upon lithiation [11], we can expect tensile stress at the surface of the Si core at the very beginning of lithiation, where the thin surface of the particle behaves similarly to a flat Si wafer [3]. The electrochemical potential at this stage is still above the lithiation potential of crystalline Si. Yet the thin silicon oxide on the surface has started lithiating, introducing tensile stress on the Si just beneath it (see Figure 4b). This results in the shift of Si Raman peak towards lower wavenumbers. The surface sensitivity of Raman makes it possible to monitor this subtle change of stress. Si usually has a native oxide layer on the surface, which contributes to the irreversible capacity loss in the first cycle of Si anodes [35,36] The tensile stress due to the lithiation of native oxide layer may be more significant in nano-structured Si anodes since their smaller radius gives larger strain for the constant displacement of the lithiated native oxide layer. Although the reaction between SiO_2 and Li has been investigated using different techniques [36], this is the first time that the stress induced by this reaction has been observed and quantified.

As soon as the Si nanoparticles start lithiating, the tensile stress gradually decreases. This indicates that an increasing compressive stress is introduced to Si (the core of the particles) when a-Li_xSi is formed on the surface, which counteracts part of the tensile stress. Upon further lithiation, the overall stress transforms from tension to compression, and its magnitude reaches ~0.3 GPa at ~6.5 h of lithiation. This result suggests the Si core is subjected to a compressive stress of 0.3 GPa at this point (see Figure 4b). The stress data during further lithiation is not available, as
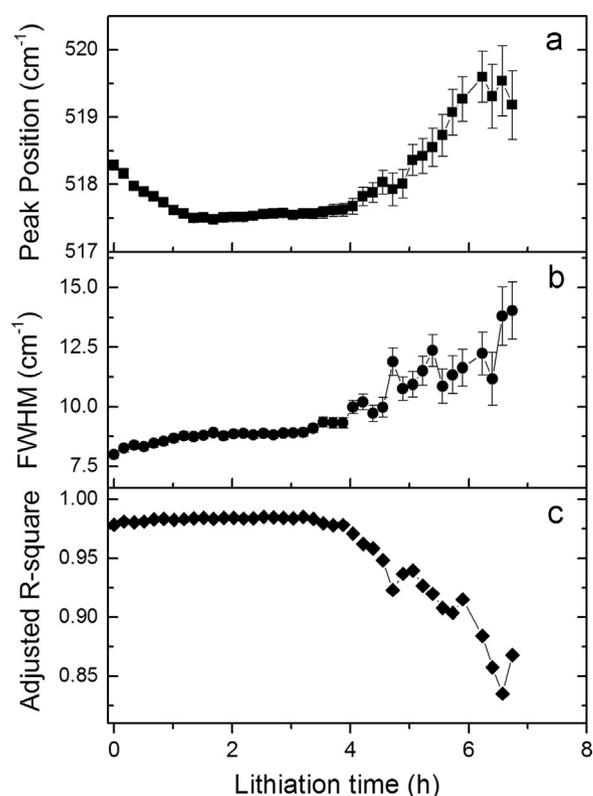

Figure 3 Position (a) and FWHM (b) of the first-order Raman peak of Si nanoparticles as a function of lithiation duration. The peaks are fit to a Voigt function. (c) Adjusted R^2 for the fit as a function of lithiation duration. A value closer to 1 indicates a better fit.

the outer layer of the particles (a-Li_xSi layer) becomes too thick, blocking most of the laser beam.

The stress evolution in Si nanoparticles has been investigated extensively by modeling [10,11,25,37]. The modeling studies rely on the knowledge of the structure evolution of Si during lithiation, which is not clear until recent in-situ TEM studies reveal its two-phase mechanism, so-called pressurized tube/hollow sphere model [30]. Herein we focus on the recent theoretical studies based on this two-phase mechanism. These studies show that during lithiation of spherical crystalline Si particles, significant tensile hoop stress can develop at the surface, while hydrostatic compression is present in the crystalline Si core [10,11,25]. And this compressive stress increases in magnitude as the core size decreases [10]. Our experiments also show an increasing compressive stress developed in the Si core of the nanoparticles during lithiation, which is consistent with the modeling results. The compression in Si core would induce a tensile stress in the a-Li_xSi shell, which likely generates cracks. This explains the experimental observation that cracks emerge at the surface of Si nanoparticles during lithiation [10,25]. In addition, we observed the stress in the Si core transformed from tension (at the very beginning of the lithiation) to compression upon further lithiation. This agrees with the modeling results of stress evolution in Si nanoparticles and Ge nanopillars during lithiation which suggest a compressive to tensile stress transition in the Li_xSi /Li_xGe layer [25,26]

The stress evolution in a Si wafer electrode has been experimentally investigated by monitoring the curvature of
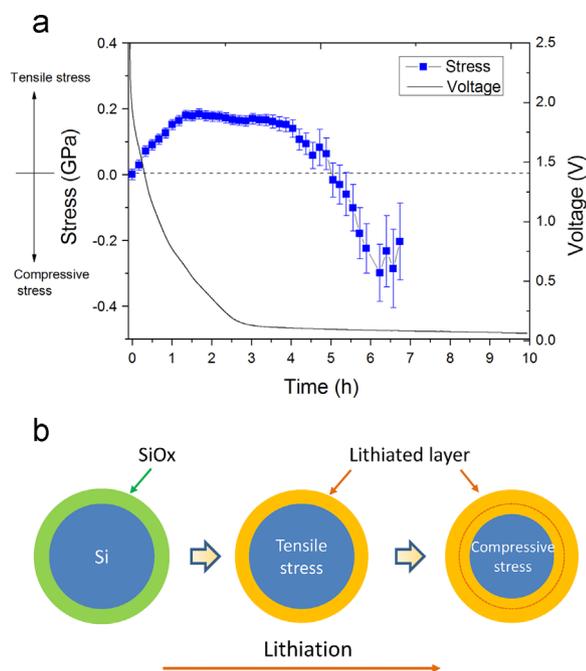
Figure 4 (a) The calculated stress in Si nanoparticles based on the measured Raman peak position as shown in Fig. 3. The corresponding voltage of the half cell is plotted as well. (b) A schematic diagram of the stress evolution in a Si nanoparticle during lithiation. The Si core experiences no stress before lithiation (left), tensile stress when oxide layer starts lithiating (middle) and compressive stress after Si starts lithiating (right). The thickness of the oxide layer is exaggerated for a better view.

the wafer using a multibeam optical sensor [3]. The stress in the a-Li$_x$Si layer was determined to be a compressive stress of ~ 0.5 GPa during lithiation, and a tensile stress up to ~ 2 GPa during de-lithiation [3]. The Li-Si reaction front is flat in the Si wafer, whereas it is curved in nanoparticles [11]. This fundamental difference may explain the different stress states observed in Si wafers compared to our work on Si nanoparticles. The fracture behavior in nanoparticles anodes also differs from that in the wafer. For Si nanoparticles and nanopillars, cracks are observed in a-Li$_x$Si during lithiation, in contrast to Si wafers where cracks are formed during delithiation [3,25,38]. This difference is well explained by their different stress states. In addition, the stress induced by the reduction of oxide layer is observed in Si nanoparticles, but not in the Si wafer. This result suggests that, compared with bulk Si, the effect of oxide surface layer is more significant in nanostructured Si anodes and it should be taken into account in theoretical studies as well.

Conclusions

In this study, we investigated the stress evolution in Si nanoparticles in-situ during lithiation using Raman spectroscopy. We found the stress in Si core of the nanoparticles transformed from tensile (0.2 GPa) to compressive (0.3 GPa) during lithiation. This experimentally observed tension-compression transition is consistent with modeling results. The stress evolution in Si nanoparticles during lithiation is quite different from that in Si wafers, indicating that the geometry and domain size of Si anodes play important roles in their stress evolution and

fracture behavior. These results provide the first quantitative experimental data of stress in nanostructured Si anodes during lithiation, and therefore offer valuable information for their computational study and rational engineering.

Acknowledgment

Appendix A. Supplementary material

Supplementary data associated with this article can be found in the online version at http://dx.doi.org/10.1016/j.nanoen.2016.02.005.

References

[1] J. Li, J.R. Dahn, J. Electrochem. Soc. 154 (2007) A156-A161.
[2] B. Key, R. Bhattacharyya, M. Morcrette, V. Seznec, J.-M. Tarascon, C.P. Grey, J. Am. Chem. Soc. 131 (2009) 9239-9249.
[3] M.J. Chon, V.A. Sethuraman, A. McCormick, V. Srinivasan, P.R. Guduru, Phys. Rev. Lett. 107 (2011) 045503.
[4] M.N. Obrovac, V.L. Chevrier, Chem. Rev. 114 (2014) 11444-11502.
[5] A. Mukhopadhyay, B.W. Sheldon, Prog. Mater. Sci. 63 (2014) 58-116.
[6] K. Rhodes, N. Dudney, E. Lara-Curzio, C. Daniel, J. Electrochem. Soc. 157 (2010) A1354-A1360.
[7] J.H. Ryu, J.W. Kim, Y.E. Sung, S.M. Oh, Electrochem. Solid-State Lett. 7 (2004) A306-A309.
[8] N.-S. Choi, K.H. Yew, K.Y. Lee, M. Sung, H. Kim, S.-S. Kim, J. Power Sources 161 (2006) 1254-1259.
[9] V.A. Sethuraman, V. Srinivasan, A.F. Bower, P.R. Guduru, J. Electrochem. Soc. 157 (2010) A1253-A1261.
[10] M.T. McDowell, I. Ryu, S.W. Lee, C. Wang, W.D. Nix, Y. Cui, Adv. Mater. 24 (2012) 6034.
[11] K. Zhao, M. Pharr, Q. Wan, W.L. Wang, E. Kaxiras, J.J. Vlassak, Z. Suo, J. Electrochem. Soc. 159 (2012) A238-A243.
[12] J. Graetz, C.C. Ahn, R. Yazami, B. Fultz, Electrochem. Solid-State Lett. 6 (2003) A194-A197.
[13] U. Kasavajjula, C. Wang, A.J. Appleby, J. Power Sources 163 (2007) 1003-1039.
[14] C.K. Chan, H.L. Peng, G. Liu, K. McIlwrath, X.F. Zhang, R. A. Huggins, Y. Cui, Nat. Nanotechnol. 3 (2008) 31-35.
[15] H. Kim, B. Han, J. Choo, J. Cho, Angew. Chem. Int. Ed. 47 (2008) 10151-10154.
[16] X. Li, M. Gu, S. Hu, R. Kennard, P. Yan, X. Chen, C. Wang, M. J. Sailor, J.-G. Zhang, J. Liu, Nat. Commun. 5 (2014).
[17] N. Liu, H. Wu, M.T. McDowell, Y. Yao, C. Wang, Y. Cui, Nano Lett. 12 (2012) 3315-3321.
[18] L.-F. Cui, R. Ruffo, C.K. Chan, H. Peng, Y. Cui, Nano Lett. 9 (2009) 491-495.
[19] H. Wu, G. Chan, J.W. Choi, I. Ryu, Y. Yao, M.T. McDowell, S. W. Lee, A. Jackson, Y. Yang, L. Hu, Y. Cui, Nat. Nanotechnol. 7 (2012) 310-315.

[20] N. Liu, Z. Lu, J. Zhao, M.T. McDowell, H.-W. Lee, W. Zhao, Y. Cui, Nat. Nano 9 (2014) 187–192.

[21] A. Magasinski, P. Dixon, B. Hertzberg, A. Kvit, J. Ayala, G. Yushin, Nat. Mater. 9 (2010) 353–358.

[22] X. Li, P. Meduri, X. Chen, W. Qi, M.H. Engelhard, W. Xu, F. Ding, J. Xiao, W. Wang, C. Wang, J.-G. Zhang, J. Liu, J. Mater. Chem. 22 (2012) 11014–11017.

[23] R. Yi, F. Dai, M.L. Gordin, S. Chen, D. Wang, Adv. Energy Mater. 3 (2012) 295–300.

[24] M. Ge, J. Rong, X. Fang, C. Zhou, Nano Lett. 12 (2012) 2318–2323.

[25] X.H. Liu, L. Zhong, S. Huang, S.X. Mao, T. Zhu, J.Y. Huang, Acs Nano 6 (2012) 1522–1531.

[26] S.W. Lee, I. Ryu, W.D. Nix, Y. Cui, Extrem. Mech. Lett. 2 (2015) 15–19.

[27] S. Misra, N. Liu, J. Nelson, S.S. Hong, Y. Cui, M.F. Toney, ACS Nano 6 (2012) 5465–5473.

[28] L.Y. Lim, N. Liu, Y. Cui, M.F. Toney, Chem. Mater. 26 (2014) 3739–3746.

[29] H.K. Mao, P.M. Bell, J.W. Shaner, D.J. Steinberg, J. Appl. Phys. 49 (1978) 3276–3283.

[30] X.H. Liu, J.W. Wang, S. Huang, F. Fan, X. Huang, Y. Liu, S. Krylyuk, J. Yoo, S.A. Dayeh, A.V. Davydov, S.X. Mao, S. T. Picraux, S. Zhang, J. Li, T. Zhu, J.Y. Huang, Nat. Nanotechnol. 7 (2012) 749–756.

[31] S. Misra, N. Liu, J. Nelson, S.S. Hong, Y. Cui, M.F. Toney, ACS Nano 6 (6) (2012) 5465–5473.

[32] B. Philippe, R. Dedryvere, J. Allouche, F. Lindgren, M. Gorgoi, H. Rensmo, D. Gonbeau, K. Edstrom, Chem. Mater. 24 (2012) 1107–1115.

[33] P. Verma, P. Maire, P. Novak, Electrochim. Acta 55 (2010) 6332–6341.

[34] P.M. Margrit Hanbucken, Ralf B. Wehrspohn (Eds.), Mechanical Stress on the Nanoscale: Simulation, Material Systems and Characterization Techniques, Wiley-VCH, Weinheim, 2011, p. 300.

[35] M.T. McDowell, S.W. Lee, I. Ryu, H. Wu, W.D. Nix, J.W. Choi, Y. Cui, Nano Lett. 11 (2011) 4018–4025.

[36] S. Xun, X. Song, L. Wang, M.E. Grass, Z. Liu, V.S. Battaglia, G. Liu, J. Electrochem. Soc. 158 (2011) A1260–A1266.

[37] R. Deshpande, Y.-T. Cheng, M.W. Verbrugge, A. Timmons, J. Electrochem. Soc. 158 (2011) A718–A724.

[38] S.W. Lee, M.T. McDowell, L.A. Berla, W.D. Nix, Y. Cui, Proc. Natl. Acad. Sci. USA 109 (2012) 4080–4085.
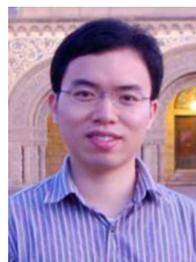
Zhidan Zeng received her B.S. degree in Materials Science and Engineering from Zhejiang University in 2006, and her Ph.D. degree in Materials Science and Engineering from Zhejiang University, China, in 2011. She is now a postdoctoral scholar in HPSynC, Geophysical Laboratory, Carnegie Institution of Washington. Her current research interests include the change of structure and properties of energy materials under pressure.


Nian Liu received his Ph.D. degree in Chemistry from Stanford University in 2014, and he is now a postdoctoral scholar with Yi Cui and Steven Chu at Stanford University. His Ph.D. research focuses on structure design of high energy battery materials. His current research interests include studying battery and other complex materials system using advanced optical techniques, as well as other topics in the intersection of nanomaterials, electrochemistry and optics. He has received 2015 Division of Inorganic Chemistry Young Investigator Award (American Chemical Society), 2014 Daniel Cubicciotti Award (The Electrochemical Society), and 2014 Chinese Government Award for Outstanding Students Abroad (China Scholarship Council).

Qiaoshi Zeng received his B.S. (2005) and Ph.D. (2010) degrees in Materials Science and Engineering from Zhejiang University, China. After his postdoctoral research at Stanford University from 2011 to 2014, he joined HPSynC, Carnegie Institution of Washington as a research scientist. He is currently a staff scientist of Center for High Pressure Science and Technology Advanced Research (HPSTAR). His research interest is mainly focused on understanding the structure and properties of amorphous materials and new materials synthesis by developing and utilizing various high pressure techniques including synchrotron radiation x-ray diffraction, imaging and spectroscopy etc.
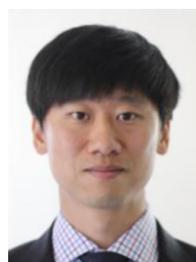
Seok Woo Lee was born in Gongju, Republic of Korea in 1981. He received his B.S. degree in mechanical engineering from Pohang University of Science and Technology (POSTECH), Pohang, Republic of Korea, in 2003 and his Ph.D. degree in mechanical engineering from Korea Advanced Institute of Science and Technology (KAIST), Daejeon, Republic of Korea, in 2008. Currently, he is a postdoctoral researcher in the Department of Materials Science and Engineering at Stanford University. He has worked on microfluidics and micro actuators using MEMS fabrication, and is currently involved in studying the mechanical behavior of silicon anodes for lithium-ion batteries.

Wendy L. Mao received her B.S. degree in Materials Science and Engineering from the Massachusetts Institute of Technology in 1998 and her Ph.D. degree in Geophysical Sciences at the University of Chicago in 2005. She became a professor in the Department of Geological Sciences at Stanford University and the Photon Science department at SLAC National Accelerator Laboratory in 2007.

Yi Cui received his B.S. degree in chemistry from the University of Science and Technology of China in 1998 and his Ph.D. degree in chemistry from Harvard University in 2002. He went on to work as a Miller Postdoctoral Fellow at the University of California, Berkeley. In 2005, he became a professor in the Department of Materials Science and Engineering at Stanford University. He leads a group of researchers working on nanomaterials for energy, environment, electronics and biology. Among many honors, he has received the Inaugural Nano Energy Award (2014), Wilson Prize from Harvard University (2011), the KAUST Investigator Award (2008), the ONR Young Investigator Award (2008), the MDV Innovators Award (2007) and the Technology Review World Top Young Innovator Award (2004).